Buoyant Magnetic Flux Tubes Enhance Radiation in *Z* Pinches

L. I. Rudakov,[1] A. L. Velikovich,[2] J. Davis,[2] J. W. Thornhill,[2] J. L. Giuliani, Jr.,[2] and C. Deeney[3]

[1]*Advanced Power Technologies, Inc., Washington, D.C. 20037*

[2]*Radiation Hydrodynamics Branch, Plasma Physics Division, Naval Research Laboratory, Washington, D.C. 20375*

[3]*Sandia National Laboratories, Albuquerque, New Mexico 87545*

(Received 18 October 1999)

In numerous experiments, magnetic energy coupled to strongly radiating Z-pinch plasmas exceeds the thermalized kinetic energy, sometimes by a factor of 2–3. We demonstrate that the enhanced energy coupling may be due to the buoyancy rise of toroidal magnetic flux tubes converging to the axis through the unstable pinch plasma. We derive an explicit formula for the enhanced dissipation rate and apply this formula to reconsider an old problem of power balance in a steady-state Z pinch, and then to analyze a new challenge of producing K-shell 3 to 10 keV radiation in long-pulse Z-pinch implosions.

PACS numbers: 52.55.Ez, 52.25.Nr, 52.50.Lp, 52.65.–y

In plasma radiation sources (PRS), Z-pinch loads are imploded to convert the magnetic energy supplied by the pulsed power driver into plasma thermal energy at stagnation, and then, finally, into x-ray radiation [1]. Numerous experiments done in the past twenty years [2–9] have established the following remarkable fact: The energy radiated by the Z-pinch plasmas can be much greater than the "mechanical" or "kinetic" or "magnetic" energy coupled to the pinch during the implosion. For many years, the energy coupling mechanism responsible for 50% or more of the observed x-ray yields remained virtually unknown.

To illustrate this, recall that the magnetic energy converted to the kinetic energy of the imploding annular plasma column is fairly estimated as

$$E_k = (aI_m^2 l/c^2)\ln(R_i/R_f) = (a/2)I_m^2 \Delta L\ \mathrm{kJ}, \quad (1)$$

where I_m [MA] is the peak current, l is the pinch length, R_i and R_f are initial and final radii, respectively, and ΔL [nH] is the change of the pinch inductance in the implosion; the dimensionless factor a accounts for the current pulse shape (typically, $a = 0.6$); all the formulas are in Gaussian units. Table I presents the kinetic energies E_k estimated from Eq. (1) and measured total x-ray yields Y for typical parameters of PRS experiments on GIT-4 in Russia [4], on Double Eagle [5], on Saturn in the short- [6] and the long-pulse regime [7,8], and on the Z generator [9]. (The data, first reported in Ref. [7], which will be published in detail elsewhere, was obtained in collaboration with Coverdale using calibrated bolometers in the same way as done for tungsten in Ref. [8].) The measured total x-ray yields in all cases are seen to be substantially larger than E_k, which is estimated from observed radial compression ratios of 6 to 25. To match the measured yields with the aid of (1), the corresponding ratios would need to be from 100 for Double Eagle and Z to 250 for GIT-4 and more than 1000 for Saturn.

Where does the additional energy come from? At stagnation, the magnetic pressure no longer performs work compressing the plasma (= pdV work). The classical Ohmic dissipation is also insufficient to generate the extra heating. For some time, it was believed to be due to anomalous resistance, although it had to be of some nonconventional kind, whose manifestation does not correlate with conditions favorable for either two-stream or ion-sound instability [10]. No theory explaining the enhanced dissipation via any kind of anomalous transport has ever been suggested.

Two recent developments indicate that the enhanced energy deposition may be a hydrodynamic (although essentially non-1D) rather than a kinetic effect. A new physical mechanism of energy dissipation in turbulent Z-pinch plasmas was proposed at the 1995 workshop on plasma turbulence in laboratory and space by Rudakov and Sudan [11]. Independently, two-dimensional (2D) numerical simulations of Z-pinch implosions (see [12] and references therein) have reproduced, without invoking anomalous resistance, "a larger drive current in the load, more energy extracted from the pulsed power system, and thus the possibility of enhanced radiation yields."

The purpose of this paper is to demonstrate that both approaches reveal the same basic mechanism of energy transfer, buoyancy-driven rise of magnetic flux tubes. Magnetic buoyancy is a very general mechanism, which works in Z pinches in a way similar to solar physics, where it is generated by sun spots and related to other forms of coronal magnetic activity, as discovered long ago by Parker

TABLE I. Typical parameters, estimated kinetic energies, and measured total x-ray yields for PRS experiments.

Generator	Material/ reference	I_m (MA)	$\frac{R_i}{R_f}$	l (cm)	E_k (kJ)	Y (kJ)
GIT-4	W [4]	1.5	6	4	10	30
DE	Ar [5]	3.5	15	4	80	140
Saturn	W [6]	6.6	20	2	157	450
	Al [7]	8	20	2	230	1060
	W [8]	8	25	2	250	750
Z	W [9]	18	25	2	1250	1800

 0031-9007/00/84(15)/3326(4)$15.00

(see [13] and references therein). This fact leads to important implications for the whole field of the Z-pinch physics, from such basic issues as energy balance of the pinch plasma or the role of its stability, to practical problems such as modeling Z-pinch implosions and developing novel PRS designs.

Recall that due to equilibrium of total pressure, $p + B^2/8\pi$, the thermal pressure p in the magnetic flux tube generated by the dynamo mechanism is lower than in the surrounding plasma, where there is no B. The temperature equilibrium implies lower plasma density ρ inside the tube. This leads to "magnetic buoyancy" [13] of the flux tube in the solar gravitational field, forcing it to rise.

Much the same happens in a Z pinch ([11], Fig. 1). Toroidal magnetic flux tubes are created at the pinch surface due to $m = 0$ modes of Rayleigh-Taylor (RT) and MHD instabilities. They are driven inward by either the magnetic buoyancy force associated with the RT instability, if the pinch is accelerated inward, or at stagnation by the curvature stress associated with the sausage MHD instability. Once the "magnetic bubble" pinches off and is completely entrained by its own current loop as a fully formed flux tube [Fig. 1(b)], it could be visualized as a contracting rubber band. As it moves to the pinch axis, magnetic flux is conserved (the band is still there), but the magnetic energy (tensile energy of the rubber) decreases, being converted to the energy of the plasma through the pdV (displacement) and the drag force work. This magnetic energy release accounts for a major contribution to the energy balance of the pinch plasma. Similarly, the temperature rise in the solar corona may be partly due to magnetic flux tubes rising through the atmosphere of the sun, and the consequent drag heating [13]. Using the conventional equations for dynamics of the thin magnetic flux tubes [11,14], let us estimate for a Z pinch the heating power associated with this process.

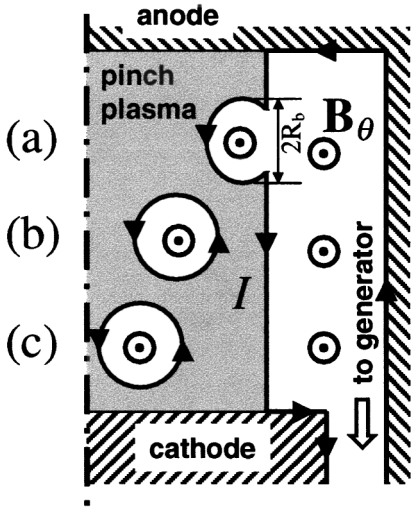

FIG. 1. (a) A magnetic bubble is formed as a $m = 0$ RT or MHD perturbation at the pinch surface. The plasma closes back behind it, producing a flux tube. (b) The flux tube is driven to the axis due to both curvature stress and buoyancy force. (c) Near the axis, it still carries the same magnetic flux, but most of its energy has been dissipated in the plasma.

Neglecting the inertia of the magnetic bubble, we find that its radial velocity ν_b is determined by the balance of the magnetic buoyancy force ρg, curvature stress $B^2/4\pi r$, and the drag force $C\rho\nu_b^2/\pi R_b$, so that $\nu_b(r) = (\pi R_b/C)^{1/2}(g + B^2/4\pi\rho r)^{1/2}$, where R_b is the smaller radius of the tube [see Fig. 1]; C is the drag coefficient (= 1 for a straight rigid cylinder at not-too-high Reynolds numbers). At the pinch boundary, $r = R$, if the buoyancy force term dominates, $g \cong I^2/\mu c^2 R$, where I and μ are the pinch current and the line mass of the pinch, respectively. At stagnation, the dominant curvature stress term $B^2/4\pi\rho R$ is estimated similarly. Therefore, in all cases $\nu_b(R) = (\pi R_b/R)^{1/2} I/c\mu^{1/2}$. The Poynting vector corresponding to the inward bubble motion equals $S = \nu_r(R)B^2/4\pi$, so that the energy is absorbed through the pinch surface area $2\pi Rl$ at the rate $P_{\rm enh} = \alpha 2\pi RlS$. Here, the coefficient $\alpha < 1$ accounts for the fraction of the pinch surface occupied by the penetrating bubbles at the late stage of the nonlinear instability development [Fig. 1(a)]. Then $P_{\rm enh} = \varsigma I^3 l/c^3\mu^{1/2}R$, where $\varsigma = 2\alpha(\pi R_b/R)^{1/2}$. Let us further assume that the processes responsible for enhanced dissipation develop in a similar way in all Z pinches. This similarity hypothesis, which implies that $\varsigma = \text{const}$, could be tested both in experiments and in simulation. For definiteness, take $\varsigma = 1/2$, as for the plausible combination of $R_b/R = 0.2$, $\alpha = 0.3$. The result is

$$P_{\rm enh} = \frac{I^3 l}{2\mu^{1/2}c^3 R} = \frac{I^3[\text{MA}]l[\text{cm}]}{2\mu^{1/2}[\mu\text{g/cm}]R[\text{mm}]}\ \text{TW}, \quad (2)$$

which corresponds to effective additional nonlinear resistance

$$\mathcal{R}_{\rm enh} = \frac{Il}{2\mu^{1/2}c^3 R} = \frac{I[\text{MA}]l[\text{cm}]}{2\mu^{1/2}[\mu\text{g/cm}]R[\text{mm}]}\ \Omega\,. \quad (3)$$

Equations (2)–(3) express the following fact, which is well established in astrophysics: "If the fluid is convectively unstable, the field rises and escapes at a rate comparable to the Alfvén speed" [13]. For a stagnated Z pinch, the role of the convective instability is played by the $m = 0$ "sausage" MHD instability.

Let us compare (2) directly with the data obtained in recent experiments and numerical simulations. In the GIT-4 tungsten experiments at $\mu = 370\ \mu$g/cm [4], substituting the observed value of $R_f = 0.42$ mm into (2) and multiplying the result by the observed confinement time, 30 ns, we obtain the enhanced energy deposition 25 kJ, quite close to the difference between Y and E_k [see Table I]. Similarly, for both short- and long-pulse experiments on Saturn with tungsten and aluminum [6–8], Eq. (2) predicts $P_{\rm enh}$ about 20 TW. More additional energy is coupled to the pinch in the long-pulse regime, when the confinement time (from ~25 ns [8] to ~30 ns [7] at $\mu = 620\ \mu$g/cm)

is longer than in the short-pulse regime (~13 ns). Multiplying 20 TW by these characteristic times, we obtain 500 to 600 kJ and 260 kJ, respectively, which in either case is close to the difference between Y and E_k in Table I.

In the Z26 shot [12,15], the peak power delivered to the pinch by the $\mathbf{J} \times \mathbf{B}$ forces, according to the simulation [12], equals 80 TW, whereas the peak power delivered to the pinch in the form of kinetic energy, dE_k/dt, is about 35 TW. The remainder, 45 TW, is close to the peak value, of pdV-generated power, 35 TW, and could be accounted for, if we substitute into (2) $\mu = 2$ mg/cm and the observed $R_f = 0.75$ mm. Then $P_{\text{enh}} = 35$ to 45 TW, for the current on Z near stagnation between 10.5 and 11.5 MA.

In another experiment on Z [15], the length of the load was decreased from 2 to 1 cm. Because of decreased inductance of the load unit, the peak current I_m increased by a factor somewhere between 1.15 and 1.34 [15]. This would decrease E_k by a factor from 0.66 to 0.9 [see (1)]. Line mass of the shortened Z-pinch load was increased by 30%, so the combined effect of length, mass, and current variations left the value (2) of P_{enh} unchanged. Likewise, the observed total x-ray yield did not decrease at all [15]. Thus some decrease in the kinetic energy in the shorter length load must have been compensated by an additional contribution from enhanced dissipation as a result of increased confinement time.

The 2D simulations demonstrate a decrease in the inductance of the imploding Z pinch compared to the 0D slug model ([12], Fig. 14), which appears to be consistent with experimental data. Since the thermodynamic free energy for arbitrary distribution of a given current I is $\tilde{\mathcal{F}} = -LI^2/2c^2$ [16], the $\mathbf{J} \times \mathbf{B}$ forces are always directed so as to increase the inductance L, thereby making $\tilde{\mathcal{F}}$ more negative. How could additional degrees of freedom in two dimensions lead to decreasing the inductance L rather than make it increase even faster? The concept of rising magnetic bubbles helps one understand this. As the bubble is formed [Fig. 1(a)], magnetic flux is supplied to it directly from the power source, and the inductance of the load increases accordingly. However, as soon as the current reconnects, and the fully formed flux tube penetrates into the pinch column, it is also disconnected from the driver [Fig. 1(b)], decreasing the volume where the driver current creates magnetic flux, and thereby decreasing the load inductance. The nonlinear resistance (3) exactly corresponds to the rate of magnetic flux losses from the driver circuit to the magnetic bubbles: $I\mathcal{R}_{\text{enh}} = (1/c)(d\Phi_b/dt)$.

We come to the conclusion of the dual role of instabilities inherent to a linear Z pinch. The RT instability at the run-in phase prevents the pinch implosion to a small final radius, and therefore has to be mitigated. Once stagnated, the pinch column "cooks" at the axis, absorbing additional magnetic energy through the enhanced dissipation mechanism essentially controlled by the MHD sausage instability. Instead of rapidly destroying the stagnated pinch plasma column, this instability actually helps to couple more energy into it, while it is "cooking" near the axis. Similar to the sun, the pinch would be "popping and boiling" [13], but can still survive as long as we manage to drive the current through it and maintain the balance between the radiative losses and the enhanced energy dissipation. For tens of nanoseconds or more, we might be able to keep coupling to the pinch plasma and converting into radiation magnetic energy already delivered to the vacuum cavity that surrounds the pinch. During this time, the $m = 0$ instability is highly active and yet does not disrupt or destroy the plasma column.

Many basic Z-pinch issues, from the Pease-Braginskii equilibrium conditions to the new problem of generation of intense K-shell radiation in the long-pulse regime, should be reconsidered in view of the above conclusion. Analysis of an energy balance between classical Ohmic heating and bremsstrahlung radiation in a steady-state Z pinch shows that the equilibrium is possible only at the so-called Pease-Braginskii current, about 1 MA [17]. Since the enhanced dissipation power (2) exceeds the classical Ohmic heating in all conditions of interest, this analysis has to be redone with the Ohmic heating power replaced by P_{enh}. We find the equilibrium to be possible for any values of current, radius, and ion charge Z:

$$\mu_{eq} = \frac{3^{3/4}\pi^{1/4}(m_e m_u)^{3/4}(c\hbar)^{1/2}(1+Z)^{1/4} I R_f^{1/2}}{2^{7/4} e^3 Z^{3/4}} = 332\,\frac{(1+Z)^{1/4}}{Z^{3/4}}\, I[\text{MA}] R_f^{1/2}[\text{mm}]\ \mu\text{g/cm}, \quad (4)$$

where m_u is atomic mass unit. For a neon plasma ($Z = 10$) cooking in an equilibrium at $I = 18$ MA, $R_f = 1$ mm, the equilibrium mass $\mu_{eq} = 1940\ \mu$g/cm corresponds to a Bennett temperature [16] of 1.58 keV, which is consistent with full ionization of neon. Similarly, to the case originally analyzed by Pease and Braginskii [17], existence of the equilibrium does not guarantee that we can organize the implosion to the final radius 1 mm in such a way that the pinch does not bounce.

Another example refers to the more efficient K-shell radiation mechanism. The pinch can be cooked near the axis for a long time, producing K-shell radiation—recent results on Saturn with Al wire array in the long-pulse regime indeed indicate that this is possible [7]. To find out whether the enhanced dissipation (2) indeed represents a sufficient energy source for producing appreciable K-shell yield, we simulated an argon pinch with the 1D radiative-MHD code described in [18]. The code was modified to include the enhanced dissipation energy source in the simplest way, by distributing the additional power (2) uniformly over the plasma mass. Our simulations were done for a constant current 4 MA and starting from a Bennett equilibrium at a 3 mm radius. We found that a low-mass column bounces, and the high-mass collapses to the axis, producing little K-shell output in both cases due to low density in the former case and low temperature in the latter. The

efficient quasi-steady conversion of magnetic energy into K-shell radiation in the cooking regime is achieved for the optimal choice of the load mass, $\mu = 200\ \mu$g/cm. Figure 2 demonstrates the pinch slowly contracting in 60 ns from the initial 3 mm radius to the final 1 mm radius. The average temperature stays close to the Bennett value, 0.83 keV. The average K-shell power maintained during the last 50 ns is about 0.8 TW/cm, which corresponds to a very substantial K-shell yield of 40 kJ/cm.

To advance further, we need a model that describes motion of the bubbles through the plasma (such as astrophysical models of [13–14]), self-consistently taking into account the plasma heating and displacement due to the bubble motion, as well as its inductance and resistance in the driving circuit. The first results in this direction are reported elsewhere [19]. The self-consistent model will help us investigate the issue of the different pinch radii observed in K-shell and L-shell emission that presently are not very well reproduced in available simulations.

Finally, we would like to highlight the fact that some of the basic physical assumptions of the mechanism outlined above could be experimentally tested by measuring the azimuthal magnetic field inside the pinch. We predict that the magnetic field does not decay near the pinch axis; rather, inside of the pinch column it remains of the same order as the field near the pinch boundary.

Another test involves directly affecting bubble formation and penetration to the axis. Suppose that for given experimental conditions the observed pinch radius at stagnation is 1 mm. Let a 1-mm radius rigid obstacle, such as a plastic or foam cylinder, nonconducting early in the implosion, be mounted at the pinch axis, in the same way as done in experiments on dynamic hohlraum [20]. Its presence would not prevent the plasma from converging to about the same final radius. However, when the pinch plasma is stagnated near the obstacle, no magnetic bubble could penetrate through the obstacle to the axis, coupling additional energy to the plasma. Our prediction is that the total x-ray yield Y will then decrease by a factor of 2 or more compared to the case when there is no obstacle. A fair estimate for Y in this case would be E_k given by Eq. (1).

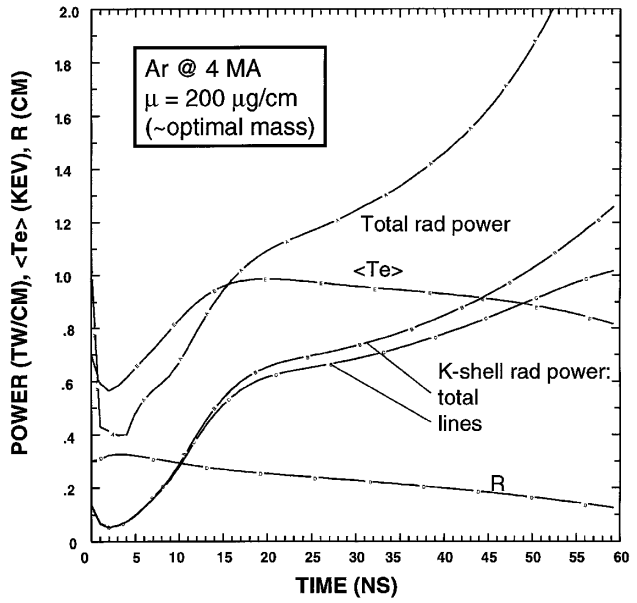

FIG. 2. Time histories of radiation power and electron temperature for an optimal mass of an argon plasma column confined for ~10 Alfvén transit times in a cooking regime.

The authors are grateful to Dr. J. P. Apruzese, Dr. K. G. Whitney, Dr. A. E. Robson, Dr. J. Chen, Dr. M. Krishnan, Dr. R. B. Baksht, Dr. I. Vitkovitsky, and Dr. D. L. Peterson for useful discussions, and to Dr. C. A. Coverdale for her contribution to the long-pulse Al radiation measurements on Saturn. This work was supported by DTRA MIPR 99-2011/1363.

[1] N. R. Pereira and J. Davis, J. Appl. Phys. **64**, R1 (1988).
[2] J. C. Riordan *et al.*, in *Sub-Kilovolt X-ray Emission from Imploding Wire Plasmas*, edited by D. Attwood and B. Henke, AIP Conf. Proc. No. 75 (AIP, New York, 1981), p. 35.
[3] M. Krishnan *et al.*, in *Dense Z-Pinches*, edited by N. R. Pereira, J. Davis, and N. Rostoker, AIP Conf. Proc. No. 195 (AIP, New York, 1989), p. 17.
[4] R. B. Baksht *et al.*, Laser Part. Beams **11**, 587 (1993).
[5] J. C. Riordan *et al.*, Bull. Am. Phys. Soc. **43**, 1905 (1998).
[6] C. Deeney *et al.*, Phys. Rev. E **56**, 5945 (1997).
[7] M. R. Douglas *et al.*, in *Proceedings of the IEEE International Conference on Plasma Science, Monterey, California, 1999, Abstracts* (IEEE, Piscataway, NJ, 1999), p. 230; C. Deeney *et al.*, *ibid.*, p. 232.
[8] C. Deeney *et al.*, Phys. Plasmas **6**, 3576 (1999).
[9] C. Deeney *et al.*, Phys. Rev. Lett. **81**, 4883 (1998).
[10] D. G. Colombant *et al.*, NRL Memorandum Report No. 3840, Naval Research Laboratory, Washington, D.C., 1978.
[11] L. I. Rudakov and R. N. Sudan, Phys. Rep. **283**, 253 (1997).
[12] D. L. Peterson *et al.*, Phys. Plasmas **5**, 3302 (1998).
[13] E. N. Parker, Astrophys. J. **121**, 491 (1955); *Cosmical Magnetic Fields* (Clarendon, Oxford, 1979).
[14] A. Ferriz-Mas and M. Schüssler, Geophys. Astrophys. Fluid Dyn. **72**, 209 (1994).
[15] R. B. Spielman *et al.*, Phys. Plasmas **5**, 2105 (1998).
[16] L. D. Landau and E. M. Lifshitz, *Electrodynamics of Continuous Media* (Pergamon, New York, 1984).
[17] R. S. Pease, Proc. Phys. Soc. London Sect. B **70**, 11 (1957); S. I. Braginskii, Sov. Phys. JETP **6**, 494 (1958).
[18] J. W. Thornhill *et al.*, J. Quant. Spectrosc. Radiat. Transfer **44**, 251 (1990).
[19] A. L. Velikovich *et al.* (to be published).
[20] T. J. Nash *et al.*, Phys. Plasmas **6**, 2023 (1999).